Asymmetric Synthesis of Unnatural α-Amino Acids through Photoredox-Mediated C–O Bond Activation of Aliphatic Alcohols

Gregory R. Alvey,[†] Elena V. Stepanova,[†,‡] Andrey Shatskiy,[†] Josefin Lantz,[†] Rachel Willemsen,[†] Alix Munoz,[†] Peter Dinér,[†] Markus D. Kärkäs[†]*

[†] Department of Chemistry, KTH Royal Institute of Technology, SE-100 44 Stockholm, Sweden

[‡] Tomsk Polytechnic University, Lenin Avenue 30, 634050 Tomsk, Russia

ABSTRACT: An efficient protocol for the asymmetric synthesis of unnatural amino acids is realized through photoredox-mediated C–O bond activation of oxalate esters derived from aliphatic alcohols as the radical precursors. The developed system uses chiral glyoxylate-derived *N*-sulfinyl imine as the radical acceptor and allows quick access to a range of functionalized unnatural amino acids through an atom-economical redox-neutral process with CO_2 as the only stoichiometric by-product.

INTRODUCTION

Unnatural amino acids (UAAs) represent a class of bioactive components with diverse applications in the pharmaceutical industry, biomedical research, and materials science.[1,2] Most commonly, UAAs serve as the building blocks for the synthesis of small-molecule drugs or as the property-modulating moieties in peptide and peptidomimetic-based medicines (Figure 1, *top*).[2] Additionally, UAA-decorated peptides are used in the development of biomaterials, biosensors, and drug delivery systems, capitalizing on the tunable non-covalent interactions in specifically designed UAA residues.[3] Furthermore, UAAs can be used for appending NMR-active or radioactive tracers to proteins, enabling detailed studies of protein function as well as medical applications, such as oncological imaging.[4,5]

The broad applicability of UAAs has stimulated the development of a multitude of (non)stereoselective approaches for their synthesis (Figure 1, *middle*).[1,6] The majority of such synthetic strategies rely on well-established reaction manifolds proceeding through closed-shell intermediates, such as asymmetric hydrogenation, electrophilic amination, Mannich and

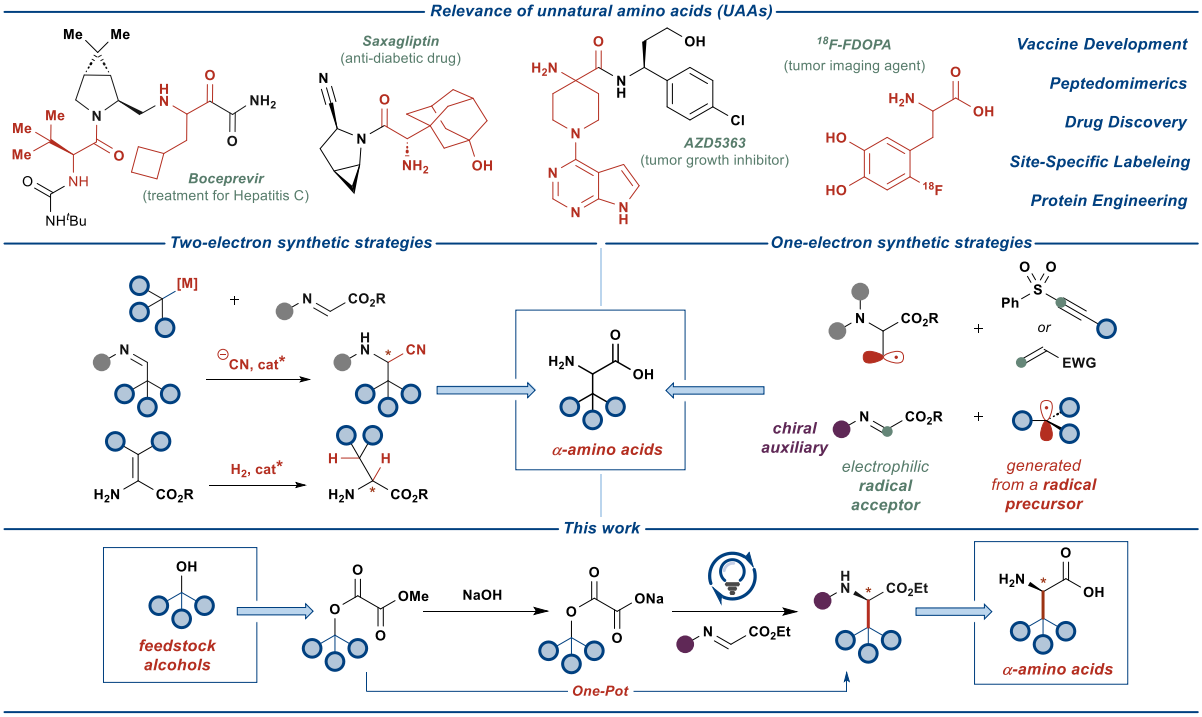

Figure 1. Relevance of unnatural amino acids (UAAs), previously developed synthetic strategies towards UUAs, and outline of the synthetic methodology proposed in this work.

Strecker-type alkylations, and Petasis borono–Mannich reaction.[7,8] In recent years, reaction manifolds featuring open-shell intermediates have also gained significant attention, prompted by the advances in photoredox catalysis[9] and electrosynthesis.[10] In these manifolds, UAAs are typically accessed through the addition of carbon-centered radicals (C-radicals) to glyoxylate imine or dehydroalanine derivatives using redox-active C-radical precursors, such as *N*-phthalimidoyl esters, trifluoroborates, amines, and others.[11,12] Alternatively, the radicals are generated at the amino acid backbone, enabling appending of redox-inactive molecules onto the amino acid side-chain.[13] Our previous work saw the entrance to such one-electron reaction manifolds with feedstock carboxylic acids as radical precursors and a chiral glyoxylate-derived *N*-sulfinyl imine as the radical acceptor.[14] The chiral-at-sulfur *N*-sulfinyl functionality served as an effective chiral auxiliary, providing β-branched UAAs with excellent stereoselectivity (>95:5 *dr*) at the α-stereogenic center. Direct oxidative activation of unfunctionalized carboxylic acids allowed realizing the developed transformation as an overall redox-neutral reaction, providing stereoselective access to a range of amino acid derivatives with high atom economy and under mild reaction conditions. In the current work, we sought

to translate this synthetic approach to a more challenging yet equally ubiquitous class of substrates — aliphatic alcohols (Figure 1, *bottom*).

Mesolytic activation of the C–O bond in aliphatic alcohols presents a formidable challenge and typically requires stoichiometric activating agents, such as phosphines and various redox-active esters and thioesters.[15,16,17] Among these, oxalate esters emerged as a prominent traceless activating group. Initially, Overman and co-workers demonstrated reductive activation of alkyl oxalates with an appended redox-active *N*-phthalimidoyl group, realizing several Giese-type radical addition reactions under photocatalytic conditions.[18,19] Significant drawbacks of these systems stemmed from the use of the additional redox-active activating group and the need for stoichiometric reducing agents, significantly limiting the applicability of such reactions. Subsequently, these drawbacks were eliminated by employing unfunctionalized alkyl oxalate salts as the radical precursors, allowing entry to the complementary redox-neutral Giese-type manifolds.[20] Under these conditions, the oxalate salts are activated through one-electron oxidation by the photocatalyst to furnish a carboxylate radical, which eliminates two molecules of CO_2 and delivers the key C-radical intermediate. Alkyl oxalate salts were successfully employed as radical precursors in numerous transformations, such as Giese-type addition reactions,[21,22,23,24] alkynylation,[25,26,27] arylation,[28,29] halogenation,[30,31,32,33] and Minisci-type manifolds,[34] as well as in total synthesis.[32,33,30,31] Additionally, these radical precursors were incorporated into several metallaphotoredox manifolds.[35,36,37,38,39] Cognizant of the versatile reactivity of alkyl oxalate salts, we sought to extend their utility to the synthesis of UAAs. Herein, we disclose a redox-neutral stereoselective strategy for constructing a diverse array of UAAs through activation of feedstock alcohols via oxalate esters.

RESULTS AND DISCUSSION

To realize the outlined traceless activation strategy, tertiary alcohol **1a** was converted to the corresponding methyl oxalate ester **2a**, followed by hydrolysis of the methyl ester functionality to furnish the model oxalate radical precursor **3a**. The model substrate **3a** was then used for optimization of the envisioned photocatalytic reaction with the chiral *N*-sulfinyl imine **4** as the radical acceptor (Figure 2). Exposing cesium oxalate salt **3a-Cs** to the photocatalytic reaction conditions optimized for the carboxylic acids as the radical

precursors[14] provided no desired product **5a** (Entry 1), presumably due to the markedly lower solubility of oxalate relative to carboxylate salts in the employed solvent ($PhCF_3$). Changing the solvent to MeCN (Entry 2) and addition of 10 equiv. of water (Entry 3) greatly increased the solubility of the oxalate radical precursor; however, only minimal amounts of the desired product were observed (11% yield, Entry 3). Gratifyingly, the screening of photoredox catalysts (Entries 3–6) revealed a sharp increase in the product yield up to 53% when utilizing $[Ir(dF(CF_3)ppy)_2(5,5'\text{-}dCF_3bpy)]PF_6$ (**PC4**) as photocatalyst (Entry 6). Alternative proton sources proved less effective than water (Entry 7) while lowering the amount of water proved marginally beneficial to the reaction (Entry 8). The screening of oxalate counterions (Entries 8–11) revealed the sodium oxalate salt as the most effective substrate, providing the desired product in 72% yield (Entry 11). Increasing the photocatalyst loading resulted in a further increase in the yield of the reaction up to 84% (Entry 12). Finally, increasing the solubility of the starting oxalate by utilizing DMF as a co-solvent delivered the desired product in an excellent yield of 92% (Entry 13). To improve the practicality of the disclosed transformation, the reaction was also conducted in a one-pot fashion with methyl oxalate ester **2a** as the substrate, demonstrating no adverse effects on the reaction outcome (92% yield, Entry 14).

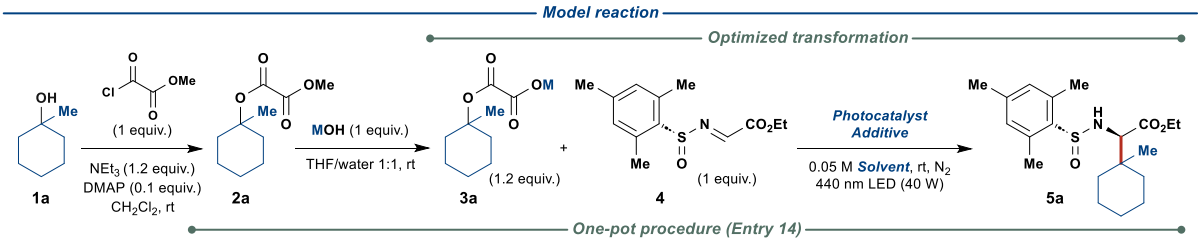

Reaction conditions

Entry	PC	PC loading	Counterion	Solvent	Additive	Time	Yield [a]
1	**PC1**	5 mol%	Cs	$PhCF_3$	–	1 h	n.d.
2	**PC1**	5 mol%	Cs	MeCN	–	1 h	n.d.
3	**PC1**	5 mol%	Cs	MeCN	10 equiv. H_2O	1 h	11%
4	**PC2**	1 mol%	Cs	MeCN	10 equiv. H_2O	1 h	n.d.
5	**PC3**	1 mol%	Cs	MeCN	10 equiv. H_2O	1 h	n.d.
6	**PC4**	1 mol%	Cs	MeCN	10 equiv. H_2O	1 h	53%
7	**PC4**	1 mol%	Cs	MeCN	10 equiv. ^tBuOH	1 h	30%
8	**PC4**	1 mol%	Cs	MeCN	5 equiv. H_2O	1 h	56%
9	**PC4**	1 mol%	NBu_4	MeCN	5 equiv. H_2O	1 h	17%
10	**PC4**	1 mol%	Li	MeCN	5 equiv. H_2O	4 h	46%
11	**PC4**	1 mol%	Na	MeCN	5 equiv. H_2O	2 h	72%
12	**PC4**	3 mol%	Na	MeCN	5 equiv. H_2O	2 h	84%
13	**PC4**	3 mol%	Na	MeCN/DMF 9:1	5 equiv. H_2O	2 h	92%
14[b]	**PC4**	**3 mol%**	**Na**	**MeCN/DMF 9:1**	**5 equiv. H_2O**	**2 h**	**92%**

Evaluated photocatalysts

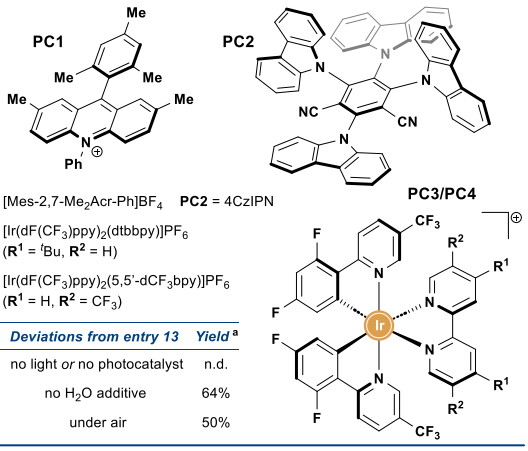

PC1 = [Mes-2,7-Me_2Acr-Ph]BF_4 **PC2** = 4CzIPN

PC3 = $[Ir(dF(CF_3)ppy)_2(dtbbpy)]PF_6$ (**R^1** = ^{t}Bu, **R^2** = H)

PC4 = $[Ir(dF(CF_3)ppy)_2(5,5'\text{-}dCF_3bpy)]PF_6$ (**R^1** = H, **R^2** = CF_3)

Entry	Deviations from entry 13	Yield [a]
15/16	no light *or* no photocatalyst	n.d.
17	no H_2O additive	64%
18	under air	50%

Figure 2. Optimization of the reaction conditions for photoredox-mediated synthesis of UAAs from aliphatic alcohols. [a] Determined by ^1H NMR using 1,3,5-trimethoxybenzene as an internal standard. [b] One-pot synthesis of **5a** from methyl oxalate ester **2a**. n.d. = not detected.

Control experiments without light (Entry 15) or photocatalyst (Entry 16) displayed no product formation, while excluding the water additive diminished the yield of the reaction down to 64% (Entry 17). Conducting the reaction open to air still provided the desired product in 50% yield (Entry 18), demonstrating a markable resilience of the disclosed protocol. Notably, all of the above reactions furnished the desired product **5a** with excellent stereoselectivity (>95:5 *dr*).

With the optimized reaction conditions (Entry 14, Figure 2), the generality of the disclosed protocol was investigated for a range of alkyl methyl oxalate substrates **2**, derived from the corresponding aliphatic alcohols **1** (Figure 3). The model tertiary oxalate substrate **2a** delivered the desired amino acid product **5a** with an excellent isolated yield of 91%. Unfortunately, all attempts to realize the disclosed transformation for simple secondary and primary alcohols, such as cyclohexanol (**1t**) and *n*-hexanol (**1q**), proved unsuccessful, and the subsequent investigation of the scope of the reaction was focused on the substrates derived from tertiary alcohols.

Carbocyclic alcohols **1b**–**h** displayed varying compatibility with the disclosed transformation. Generally, higher isolated yields were observed for less sterically-encumbered substrates, such as **2b**, **2f** and **2g** (44–62% yields), while complex polycyclic substrates **2d** and **2e** were less effective, providing products **5d** and **5e** in 22% and 33% yields, respectively. Contrary to this trend, bicyclo[3.1.1]heptane-containing substrate **2h** and 2-indanol-based substrate **2c** provided the respective amino acid products in 77% and 18% isolated yields. Acyclic tertiary oxalate substrates **2i** and **2j** provided the desired products in good and excellent yields of 67% and 90%, respectively, while the related chloride-substituted substrate **2k** was less effective (22% yield). Intriguingly, the terminal alkene–containing substrate **2l** and the primary alcohol substrate **2m** successfully delivered the respective products, albeit in moderate yields (46% and 33%, respectively). To further investigate the functional group compatibility of the disclosed transformation, we prepared a series of functionalized oxalate substrates **2n**–**s** derived from 3-methyl-1,3-butanediol. The primary alcohol functionality in this diol was selectively decorated with various functional groups, while the tertiary alcohol group was activated as the methyl oxalate ester. Gratifyingly, silyl ether (**2n**), benzoate (**2o**), nicotinate (**2q**), 2-thiophenecarboxylate (**2r**), and glycoside (**2s**) diol-derived substrates provided the expected amino acid products in good to excellent yields (58–88%). As expected, bromine-

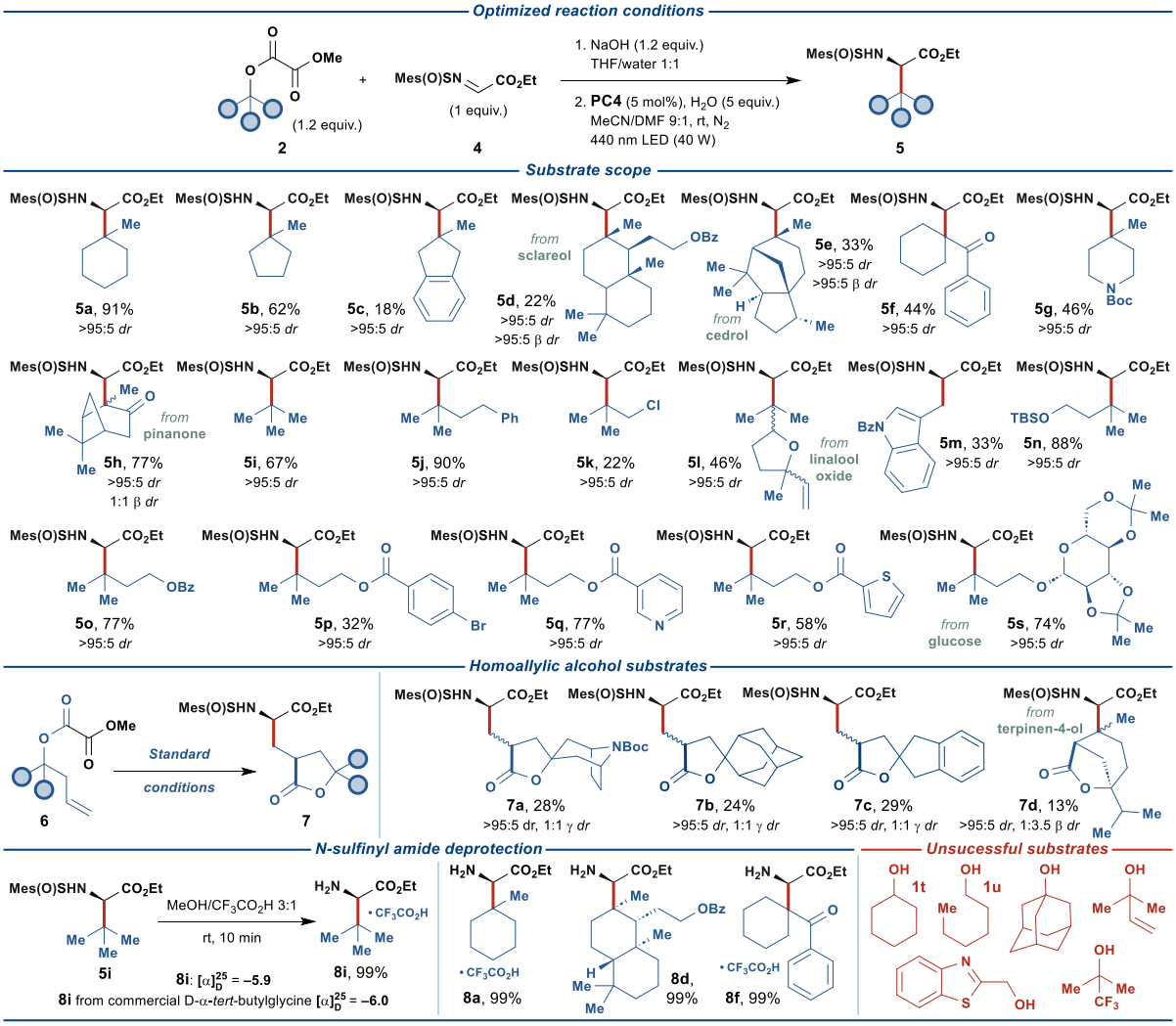

Figure 3. Substrate scope of photoredox-mediated synthesis of UAAs **5** and **7** and deprotection of the *N*-sulfinyl amide-functionalized products **5**. Isolated product yields are reported.

containing substrate **2p** proved less effective and delivered the amino acid product **5p** in 32% yield. Inspired by the previously developed photocatalytic systems featuring oxalate activating group,[40] we investigated several substrates derived from homoallylic alcohols **6**. For such substrates, elimination of the second CO_2 molecule from the one-electron oxidized oxalate (vide supra) is outcompeted by the intramolecular radical addition of the transient oxyacyl radical to the double bond. The resulting primary C-radical then undergoes addition to *N*-sulfinyl imine **4** to furnish γ-branched amino acid products **7**. The carbocyclic homoallylic substrates **6a**–**c** engaged in the reaction to provide synthetically challenging spirocyclic products **7a**–**c**, albeit in relatively low yields (24–29%). Interestingly, a substrate containing an endocyclic alkene functionality **6d** could still provide a bicyclic cyclization/radical addition product **7d** in 13% yield, despite unfavorable sterical characteristics (cf. product **5e**).

To conclude, while displaying suboptimal yields for some products, the disclosed transformation proved compatible with a range of structural motives and functional groups, such as ketone, ketal, *N*-*tert*-butyloxycarbonyl, alkenyl, silyl ether, aromatic esters, pyridine, thiophene, and indole. Additionally, several biologically-relevant substrates derived from sclareol, cedrol, pinanone, linalool oxide, glucose, and terpinene were compatible with the developed protocol. Excellent diastereoselectivity was observed for the α-stereogenic center (>95:5 *dr*) in all of the produced amino acid products, while the sterically encumbered products **5d** and **5e** also displayed excellent diastereoselectivity at the β-stereogenic center (>95:5 β *dr*).

The practicality of the developed protocol was highlighted through the straightforward removal of the chiral auxiliary. The *N*-sulfinyl group was removed from the amino acid adducts **5a**, **5d**, **5f**, and **5i** under mildly acidic conditions, providing the respective amino acid products **8** in quantitative isolated yields. Comparing the specific optical rotation for product **8i** and the corresponding commercial amino acid derivative revealed full retention of the α-stereogenic center in **8i** during *N*-sulfinyl deprotection and confirmed the proposed absolute configuration of the product (*R*).

Based on the literature precedents, a plausible mechanism for the disclosed transformation was proposed (Figure 4, *top*).[23,14,40] The photocatalytic cycle is onset by excitation of the photocatalyst **PC** by blue light ($\lambda \approx 440$ nm), followed by quenching of the excited-state photocatalyst **PC*** by oxalate ester salt **3** through single-electron transfer (SET). This step furnishes a reduced ground-state photocatalyst $\mathbf{PC^{red}}$ and carboxylate radical **9**, which readily eliminates CO_2 to form oxyacyl radical **10**. The latter eliminates the second molecule of CO_2 to produce the key C-radical intermediate **11**. This radical engages in the stereodetermining C–C bond-forming step with *N*-sulfinyl imine **4**, furnishing *N*-radical intermediate **12**. As has been detailed previously,[14] the stereochemical outcome of this step is defined by the conformation of the radical acceptor **4**, which is set by intramolecular hydrogen bonding between the α-C–H hydrogen and the O-atom of the sulfone moiety. Finally, intermediate **12** transforms into the desired product **5** upon SET from the reduced photocatalyst $\mathbf{PC^{red}}$ and protonation from solvent, concluding the photocatalytic cycle. Oxalate ester substrates **6** derived from homoallylic alcohols follow a complementary mechanistic pathway (Figure 4, *top right*). For

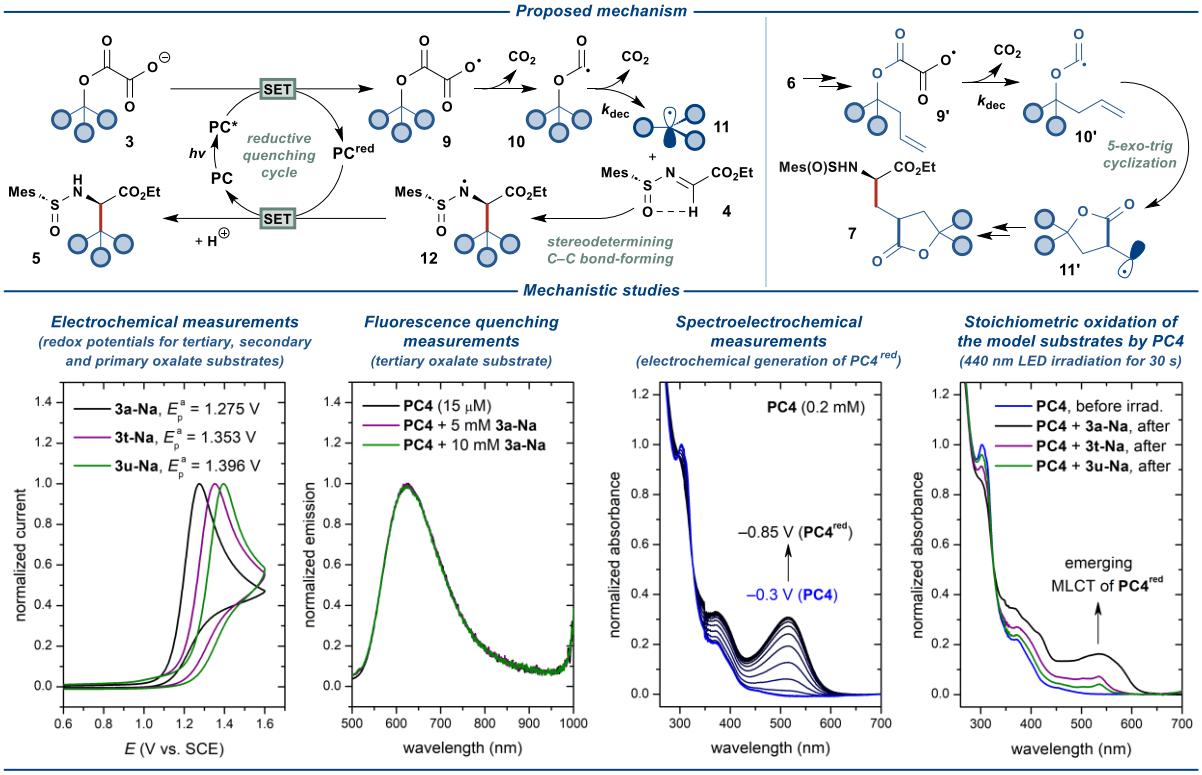

Figure 4. Proposed mechanism for the developed transformation and the mechanistic studies (for details, see the Supplementary Information).

this class of substrates, elimination of CO_2 from oxyacyl radical **10'** is outcompeted by 5-*exo*-*trig* cyclization to furnish a primary C-radical **11'**, which subsequently engages in the key C–C bond-forming reaction with **4** to deliver the lactone-containing amino acid product **7**.

The feasibility of the outlined mechanism and the observed reactivity patterns were investigated with a series of spectroscopical, electrochemical and computational studies (Figure 4, *bottom*). The oxalate ester salt **3a-Na** displayed sufficiently low oxidation potential (E_{pa} = 1.28 V; all potentials are specified vs. SCE) to quench the excited states of all of the evaluated oxidizing photocatalysts (**PC1**–**PC4**, $E(PC^*/PC^{red}$ ≈ 1.2–2.1 V).[41,42,43,44,45] However, only photocatalyst **PC4** effectively promoted the desired reaction. Similar to the previously described decarboxylative photocatalytic system,[14] **PC2** and **PC3** are likely unsuitable due to the considerably low oxidation potentials of their reduced state ($E(PC/PC^{red})$ = –1.21 V and –1.37 V, respectively), leading to deleterious one-electron reduction of the imine substrate **4** (E_{pc} = –1.34 V). The increased oxidation potentials for **PC1** and **PC4** ($E(PC/PC^{red})$ = –0.58 V and –0.69 V, respectively) allow avoiding such reductive side-reaction. While **PC1** proved highly effective for the decarboxylative synthesis of UAAs from carboxylate salts,[14] it could only

promote the reaction with $PhCF_3$ as the solvent. The lower solubility of oxalate relative to carboxylate salts in $PhCF_3$ is likely to be behind the impeded reactivity of **PC1** for decarboxylative activation of oxalate ester salts.

To our surprise, the steady-state fluorescence quenching experiments displayed no quenching of the excited-state **PC4** by the model substrate **3a-Na** (Figure 4, *bottom*). Thereby, we sought to support the outlined reductive quenching cycle through alternative stoichiometric experiments. Electroreduction of **PC4** in a spectroelectrochemical cell upon sweeping the potential of the working electrode from –0.3 V to –0.85 V resulted in the gradual appearance of an MLCT absorption band (λ_{max} = 515 nm), as expected for reduction of an Ir(III) polypyridyl complex to the Ir(II) state (**PC4**^{red}). Gratifyingly, the formation of a similar absorption band (λ_{max} = 535 nm) was observed for the solution of **PC4** in the presence of **3a** after 30 s of irradiation with 440 nm LED, supporting the proposed reductive quenching cycle. Conducting the same experiments with the oxalates derived from secondary (**1t**) and primary alcohols (**1q**) displayed the highly impeded ability of these substrates to engage in electron transfer with **PC4**. This observation is in agreement with the increased oxidation potentials for these substrates (E_{pa} ≈ 1.35 V and 1.40 V for **3t-Na** and **3u-Na**, respectively). Therefore, the primary factor precluding the use of secondary and primary alcohol substrates in the disclosed transformation is the unfavorable oxidative SET. As has been proposed previously,[24] the secondary factor for the decreased reactivity is likely the reduced rate constant for decarboxylation of the respective oxyacyl radicals **10** ($k_{dec} \approx 10^5$ s^{-1} and 10^2 s^{-1} for the oxalates derived from tertiary and secondary/primary alcohols, respectively).[46] This trend was confirmed by computational studies with *tert*-butanol, *iso*-propanol, and ethanol-derived oxalates as the model substrates (for details, see the Supplementary Information). At the same time, only minimal differences in activation barriers were found for the other steps of the proposed mechanism for the tertiary, secondary, and primary model substrates.

CONCLUSIONS

The developed photocatalytic system allows straightforward access to a diverse set of unnatural amino acids using ubiquitous alcohols as the radical precursors, which are activated through photoinduced oxidation of the corresponding alkyl oxalate esters. Utilizing homoallylic alcohols as substrates further extends the scope of the disclosed protocol to

encompass synthetically challenging spirocyclic lactone–decorated amino acids. The mechanistic studies highlight the intricate dependence of the reaction efficiency on the nature of the alcohol substrates.

ACKNOWLEDGEMENTS

Financial support to M.D.K. from FORMAS (grant no. 2019-01269), the Swedish Research Council (grant no. 2020-04764), the Magnus Bergvall Foundation, Olle Engkvist Foundation, and KTH Royal Institute of Technology is gratefully acknowledged. Financial support to E.V.S. from the Russian Science Foundation (project no. 21-73-10211) is gratefully acknowledged. The National Supercomputer Center (NSC) in Linköping is acknowledged for providing computational resources.

AUTHOR CONTRIBUTIONS

Conceptualization: M.D.K. Optimization and substrate scope: G.R.A., E.V.S., A.S., J.L., R.W., A.M. Experimental mechanistic studies: A.S. Computational studies: P.D. Funding acquisition: E.V.S., M.D.K. Supervision: M.D.K. Writing and editing of the manuscript: G.R.A., E.V.S., A.S., M.D.K.

DECLARATION OF INTERESTS

The authors declare no competing interests.

REFERENCES

1. Narancic, T., Almahboub, S.A., and O'Connor, K.E. (2019). Unnatural amino acids: production and biotechnological potential. World J. Microbiol. Biotechnol. *35*, 67. https://doi.org/10.1007/s11274-019-2642-9
2. Blaskovich, M.A.T. (2016). Unusual Amino Acids in Medicinal Chemistry. J. Med. Chem. *59*, 10807–10836. https://doi.org/10.1021/acs.jmedchem.6b00319
3. Huo, Y., Hu, J., Yin, Y., Liu, P., Cai, K., and Ji, W. (2023). Self-Assembling Peptide-Based Functional Biomaterials. ChemBioChem *24*, e202200582. https://doi.org/10.1002/cbic.202200582

4. Seifert, M.H.J., Ksiazek, D., Azim, M.K., Smialowski, P., Budisa, N., and Holak, T.A. (2002). Slow Exchange in the Chromophore of a Green Fluorescent Protein Variant. J. Am. Chem. Soc. *124*, 7932–7942. https://doi.org/10.1021/ja0257725

5. Qi, Y., Liu, X., Li, J., Yao, H., and Yuan, S. (2017). Fluorine-18 labeled amino acids for tumor PET/CT imaging. Oncotarget *8*, 60581–60588. https://doi.org/10.18632/oncotarget.19943

6. Adhikari, A., Bhattarai, B.R., Aryal, A., Thapa, N., Kc, P., Adhikari, A., Maharjan, S., Chanda, P.B., Regmi, B.P., and Parajuli, N. (2021). Reprogramming natural proteins using unnatural amino acids. RSC Adv. *11*, 38126–38145. https://doi.org/10.1039/D1RA07028B

7. Ma, J.-A. (2003). Recent Developments in the Catalytic Asymmetric Synthesis of α- and β-Amino Acids. Angew. Chem. Int. Ed. *42*, 4290–4299. https://doi.org/10.1002/anie.200301600

8. Nájera, C., and Sansano, J.M. (2007). Catalytic Asymmetric Synthesis of α-Amino Acids. Chem. Rev. *107*, 4584–4671. https://doi.org/10.1021/cr050580o

9. Shaw, M.H., Twilton, J., and MacMillan, D.W.C. (2016). Photoredox Catalysis in Organic Chemistry. J. Org. Chem. *81*, 6898–6926. https://doi.org/10.1021/acs.joc.6b01449

10. Zhu, C., Ang, N.W.J., Meyer, T.H., Qiu, Y., and Ackermann, L. (2021). Organic Electrochemistry: Molecular Syntheses with Potential. ACS Cent. Sci. *7*, 415–431. https://doi.org/10.1021/acscentsci.0c01532

11. Shatskiy, A., and Kärkäs, M.D. (2022). Photoredox-Enabled Decarboxylative Synthesis of Unnatural α-Amino Acids. Synlett *33*, 109–115. https:// doi.org/10.1055/a-1499-8679

12. Wang, M., Wang, C., Huo, Y., Dang, X., Xue, H., Liu, L., Chai, H., Xie, X., Li, Z., Lu, D., et al. (2021). Visible-light-mediated catalyst-free synthesis of unnatural α-amino acids and peptide macrocycles. Nat. Commun. *12*, 6873. https://doi.org/10.1038/s41467-021-27086-x

13. Jiang, M., Jin, Y., Yang, H., and Fu, H. (2016). Visible-light photoredox synthesis of unnatural chiral α-amino acids. Sci. Rep. *6*, 26161. https://doi.org/10.1038/srep26161

14. Shatskiy, A., Axelsson, A., Stepanova, E.V., Liu, J.-Q., Temerdashev, A.Z., Kore, B.P., Blomkvist, B., Gardner, J.M., Dinér, P., and Kärkäs, M.D. (2021). Stereoselective synthesis of unnatural α-amino acid derivatives through photoredox catalysis. Chem. Sci. *12*, 5430–5437. https://doi.org/10.1039/D1SC00658D

15. Anwar, K., Merkens, K., Aguilar Troyano, F.J., and Gómez-Suárez, A. (2022). Radical Deoxyfunctionalisation Strategies. Eur. J. Org. Chem. *2022,* p.e202200330. https://doi.org/10.1002/ejoc.202200330

16. Villo, P., Shatskiy, A., Kärkäs, M.D., and Lundberg, H. (2023). Electrosynthetic C−O Bond Activation in Alcohols and Alcohol Derivatives. Angew. Chem. Int. Ed. *62*, e202211952. https://doi.org/10.1002/anie.202211952

17. Hu, X.-Q., Hou, Y.-X., Liu, Z.-K., and Gao, Y. (2020). Recent advances in phosphoranyl radical-mediated deoxygenative functionalisation. Org. Chem. Front. *7*, 2319–2324. https://doi.org/10.1039/D0QO00643B

18. Lackner, G.L., Quasdorf, K.W., and Overman, L.E. (2013). Direct Construction of Quaternary Carbons from Tertiary Alcohols via Photoredox-Catalyzed Fragmentation of *tert*-Alkyl *N*-Phthalimidoyl Oxalates. J. Am. Chem. Soc. *135*, 15342–15345.https://doi.org/10.1021/ja408971t

19. Lackner, G.L., Quasdorf, K.W., Pratsch, G., and Overman, L.E. (2015). Fragment Coupling and the Construction of Quaternary Carbons Using Tertiary Radicals Generated From *tert*-Alkyl *N*-Phthalimidoyl Oxalates By Visible-Light Photocatalysis. J. Org. Chem. *80*, 6012–6024. https://doi.org/10.1021/acs.joc.5b00794

20. Nawrat, C.C., Jamison, C.R., Slutskyy, Y., MacMillan, D.W.C., and Overman, L.E. (2015). Oxalates as Activating Groups for Alcohols in Visible Light Photoredox Catalysis: Formation of Quaternary Centers by Redox-Neutral Fragment Coupling. J. Am. Chem. Soc. *137*, 11270–11273. https://doi.org/10.1021/jacs.5b07678

21. Wang, Q., Yue, L., Bao, Y., Wang, Y., Kang, D., Gao, Y., and Yuan, Z. (2022). Oxalates as Activating Groups for Tertiary Alcohols in Photoredox-Catalyzed *gem* -Difluoroallylation To Construct All-Carbon Quaternary Centers. J. Org. Chem. *87*, 8237–8247. https://doi.org/10.1021/acs.joc.2c00664

22. Abbas, S.Y. (2021). Addition of the tertiary radicals to electron-deficient 1,3-dienes using photoredox catalysis. Journal of Photochemistry and Photobiology A: Chemistry *418*, 113434. https://doi.org/10.1016/j.jphotochem.2021.113434

23. Abbas, S.Y., Zhao, P., and Overman, L.E. (2018). 1,6-Addition of Tertiary Carbon Radicals Generated From Alcohols or Carboxylic Acids by Visible-Light Photoredox Catalysis. Org. Lett. *20*, 868–871. https://doi.org/10.1021/acs.orglett.7b04034

24. Sun, W., Zou, J., Xu, X., Wang, J., Liu, M., and Liu, X. (2022). Photo-Catalyzed Redox-Neutral 1,2-Dialkylation of Alkenes. Adv. Synth. Catal. 364, 2260–2265. https://doi.org/10.1002/adsc.202200310

25. Li, M., Liu, T., Li, J., He, H., Dai, H., and Xie, J. (2021). Visible-Light-Mediated Deoxyalkynylation of Activated Tertiary Alcohols. J. Org. Chem. *86*, 12386–12393. https://doi.org/10.1021/acs.joc.1c01356

26. Amos, S.G.E., Le Vaillant, F., and Waser, J. (2023). Exploring Photoredox-Catalyzed (Re)functionalizations with Core-Modified Benziodoxolones. Helvetica Chimica Acta *106,* e202200161. https://doi.org/10.1002/hlca.202200161

27. Amos, S.G.E., Cavalli, D., Le Vaillant, F., and Waser, J. (2021). From Photoredox Catalysis to the Direct Excitation of EthynylBenziodoXolones: Accessing Alkynylated Quaternary Carbons from Alcohols via Oxalates. ChemRxiv. https://doi.org/10.26434/chemrxiv-2021-56f12

28. Lipp, B., Nauth, A.M., and Opatz, T. (2016). Transition-Metal-Free Decarboxylative Photoredox Coupling of Carboxylic Acids and Alcohols with Aromatic Nitriles. J. Org. Chem. *81*, 6875–6882. https://doi.org/10.1021/acs.joc.6b01215

29. Pitre, S.P., Muuronen, M., Fishman, D.A., and Overman, L.E. (2019). Tertiary Alcohols as Radical Precursors for the Introduction of Tertiary Substituents into Heteroarenes. ACS Catal. *9*, 3413–3418. https://doi.org/10.1021/acscatal.9b00405

30. Aguilar Troyano, F.J., Ballaschk, F., Jaschinski, M., Özkaya, Y., and Gómez-Suárez, A. (2019). Light-Mediated Formal Radical Deoxyfluorination of Tertiary Alcohols through Selective Single-Electron Oxidation with $TEDA^{2+\cdot}$ Chem. Eur. J. *25*, 14054–14058. https://doi.org/10.1002/chem.201903702

31. González-Esguevillas, M., Miró, J., Jeffrey, J.L., and MacMillan, D.W.C. (2019). Photoredox-catalyzed deoxyfluorination of activated alcohols with Selectfluor®. Tetrahedron *75*, 4222–4227. https://doi.org/10.1016/j.tet.2019.05.043

32. Brioche, J. (2018). One-pot synthesis of tertiary alkyl fluorides from methyl oxalates by radical deoxyfluorination under photoredox catalysis. Tetrahedron Letters *59*, 4387–4391. https://doi.org/10.1016/j.tetlet.2018.10.063

33. Su, J.Y., Grünenfelder, D.C., Takeuchi, K., and Reisman, S.E. (2018). Radical Deoxychlorination of Cesium Oxalates for the Synthesis of Alkyl Chlorides. Org. Lett. 20, 4912–4916. https://doi.org/10.1021/acs.orglett.8b02045

34. Dong, J., Wang, Z., Wang, X., Song, H., Liu, Y., and Wang, Q. (2019). Metal-, Photocatalyst-, and Light-Free Minisci C–H Alkylation of N -Heteroarenes with Oxalates. J. Org. Chem. 84, 7532–7540. https://doi.org/10.1021/acs.joc.9b00972

35. Zhang, X., and MacMillan, D.W.C. (2016). Alcohols as Latent Coupling Fragments for Metallaphotoredox Catalysis: sp^3–sp^2 Cross-Coupling of Oxalates with Aryl Halides. J. Am. Chem. Soc. *138*, 13862–13865. https://doi.org/10.1021/jacs.6b09533

36. Guo, L., Song, F., Zhu, S., Li, H., and Chu, L. (2018). syn-Selective alkylarylation of terminal alkynes via the combination of photoredox and nickel catalysis. Nat. Commun. *9*, 4543. https://doi.org/10.1038/s41467-018-06904-9

37. Guo, L., Tu, H.-Y., Zhu, S., and Chu, L. (2019). Selective, Intermolecular Alkylarylation of Alkenes via Photoredox/Nickel Dual Catalysis. Org. Lett. *21*, 4771–4776. https://doi.org/10.1021/acs.orglett.9b01658

38. Li, W.-D., Jiang, Y.-Q., Li, Y.-L., and Xia, J.-B. (2022). Photoredox Ni-Catalyzed Selective Coupling of Organic Halides and Oxalates to Esters via Alkoxycarbonyl Radical Intermediates. CCS Chem *4*, 1326–1336. https://doi.org/10.31635/ccschem.021.202100920

39. Li, H., Guo, L., Feng, X., Huo, L., Zhu, S., and Chu, L. (2020). Sequential C–O decarboxylative vinylation/C–H arylation of cyclic oxalates *via* a nickel-catalyzed multicomponent radical cascade. Chem. Sci. *11*, 4904–4910. https://doi.org/10.1039/D0SC01471K

40. Weires, N.A., Slutskyy, Y., and Overman, L.E. (2019). Facile Preparation of Spirolactones by an Alkoxycarbonyl Radical Cyclization–Cross-Coupling Cascade. Angew. Chem. Int. Ed. *58*, 8561–8565. https://doi.org/10.1002/anie.201903353

41. Wilger, D.J., Grandjean, J.-M.M., Lammert, T.R., and Nicewicz, D.A. (2014). The direct anti-Markovnikov addition of mineral acids to styrenes. Nature Chem. *6*, 720–726. https://doi.org/10.1038/nchem.2000

42. Luo, J., and Zhang, J. (2016). Donor–Acceptor Fluorophores for Visible-Light-Promoted Organic Synthesis: Photoredox/Ni Dual Catalytic $C(sp^3)$–$C(sp^2)$ Cross-Coupling. ACS Catal. *6*, 873–877. https://doi.org/10.1021/acscatal.5b02204

43. Lowry, M.S., Goldsmith, J.I., Slinker, J.D., Rohl, R., Pascal, R.A., Malliaras, G.G., and Bernhard, S. (2005). Single-Layer Electroluminescent Devices and Photoinduced Hydrogen Production from an Ionic Iridium(III) Complex. Chem. Mater. *17*, 5712–5719. https://doi.org/10.1021/cm051312+

44. Lowry, M.S., Goldsmith, J.I., Slinker, J.D., Pascal, R.A., Malliaras, G.G., and Bernhard, S. (2023). Correction to Single-Layer Electroluminescent Devices and Photoinduced Hydrogen Production from an Ionic Iridium(III) Complex. Chem. Mater. *35*, 1466–1466. https://doi.org/10.1021/acs.chemmater.2c03710

45. Choi, G.J., Zhu, Q., Miller, D.C., Gu, C.J., and Knowles, R.R. (2016). Catalytic alkylation of remote C–H bonds enabled by proton-coupled electron transfer. Nature *539*, 268–271. https://doi.org/10.1038/nature19811

46. Simakov, P.A., Martinez, F.N., Horner, J.H., and Newcomb, M. (1998). Absolute Rate Constants for Alkoxycarbonyl Radical Reactions. J. Org. Chem. *63*, 1226–1232. https://doi.org/10.1021/jo971774+